# Isothermal Kinetic Study of Nitric Oxide Adsorption and Decomposition on Pd(111) Surfaces: Molecular Beam Experiments

**Kandasamy Thirunavukkarasu,[†] Krishnan Thirumoorthy,[†] Jörg Libuda,[‡] and Chinnakonda S. Gopinath*[,†]**

*Catalysis Division, National Chemical Laboratory, Dr. Homi Bhabha Road, Pune 411 008, India, and Department of Chemical Physics, Fritz-Haber-Institut der Max-Planck-Gesellschaft, Faradayweg 4−6, 14195 Berlin, Germany*

*Received: February 16, 2005; In Final Form: May 30, 2005*

The kinetics of NO adsorption and dissociation on Pd(111) surfaces and the NO sticking coefficient ($s_{NO}$) were probed by isothermal kinetic measurements between 300 and 525 K using a molecular beam instrument. NO dissociation and $N_2$ productions were observed in the transient state from 425 K and above on Pd(111) surfaces with selective nitrogen production. Maximum nitrogen production was observed between 475 and 500 K. It was found that, at low temperatures, between 300 and 350 K, molecular adsorption occurs with a constant initial $s_{NO}$ of 0.5 until the Pd(111) surface is covered to about 70−80% by NO. Then $s_{NO}$ rapidly decreases with further increasing NO coverage, indicating typical precursor kinetics. The dynamic adsorption − desorption equilibrium on Pd(111) was probed in modulated beam experiments below 500 K. CO titration experiments after NO dosing indicate the diffusion of oxygen into the subsurface regions and beginning surface oxidation at ≥475 K. Finally, we discuss the results with respect to the rate-limiting character of the different elementary steps of the reaction system.

## 1. Introduction

In the last 2 decades increasing governmental regulations all over the world have stimulated tremendous growth in the research on environmental catalysis and green chemistry.[1−3] In particular, the automotive catalyst technology has improved, assisted by better petrochemical refining to yield cleaner fuels. Improvements in internal combustion engines and the above developments have led to fuel-efficient vehicles. The present technology of three-way catalytic converters[1,2] meets the requirements of oxidation of CO. More problematic is the oxidation of nonvolatile organic species to $CO_2$ and, in particular, the reduction of NO to $N_2$, especially under the highly oxidizing exhaust gas conditions of fuel-efficient lean-burn engines.[4] Although Rh is very active for NO reduction under fuel-rich conditions, this is not the case under net oxidizing conditions, since the excess oxygen inhibits the NO reduction activity of Rh by oxidizing it. Pd has also been added to catalytic converters as one of the active metals for NO reduction for the past few years;[5] however, the mechanistic details of Pd are not fully understood yet. There were few new technologies[6,7] introduced in the past decade, like $NO_x$ storage or zeolite based catalysts, which provided different insights into the NO reduction. However, regarding long-term stability, low and high-temperature NO reduction is still a challenge.[4] The above points clearly indicates that there is an urgent need to develop catalysts for NO reduction under net oxidizing conditions. In this respect, obtaining molecular-level insights into underlying catalysis aspects of NO reduction is a major challenge for current research.

Palladium has been suggested as an alternative active element for NO reduction due to its NO dissociation capacity and its stability under high temperature and oxidizing conditions.[8−10] However, unlike Rh,[11−15] Pd has not been subjected to intense research, and its capability for NO reduction is not fully understood. In the recent past, there have been numerous reports on the NO reduction over Pd-based catalysts on different faces of single crystals and a variety of supported systems.[16−29] Despite that, there is a lack of fundamental understanding of NO reduction on the Pd surfaces.

The present work of NO adsorption and dissociation on Pd-(111) focuses on fundamental kinetic aspects under isothermal conditions in a molecular beam instrument.[30−34] It was suggested that NO dissociates only at defect sites on Pd(111) without significant inherent activity on Pd(111);[17−20] nonetheless, there are reports[22−26,28,29,35] on steady-state NO dissociation to $N_2$ and $N_2O$ on Pd(111) as well as on Pd on supported oxides with reductants, like CO and $H_2$, indicating inherent catalytic activity toward NO dissociation. Our present studies show that an inherent NO dissociation activity exists on Pd(111) surfaces, and the same can be observed clearly in the transient state. The present work on the dissociation of NO on Pd(111) surfaces is a part of our continuing study of the NO reduction reactions in our laboratory, and the NO + CO reaction on Pd(111) is reported in ref 35.

## 2. Experimental Section

All kinetic and TPD experiments reported in this manuscript were performed using an extension of the so-called King and Wells collimated beam method. The home-built molecular beam instrument (MBI) used consists a 12 L capacity stainless steel ultrahigh vacuum (UHV) chamber evacuated with a 210 L/s turbo-molecular drag pump (Pfeiffer, TMU261) to a base pressure of about $3 \times 10^{-10}$ Torr. The MBI is equipped with a

* Corresponding author. E-mail: cs.gopinath@ncl.res.in. Fax: 0091-20-2589 3761.
[†] National Chemical Laboratory.
[‡] Fritz-Haber-Institut der Max-Planck-Gesellschaft.

10.1021/jp050813f CCC: $30.25 
Published on Web 06/21/2005

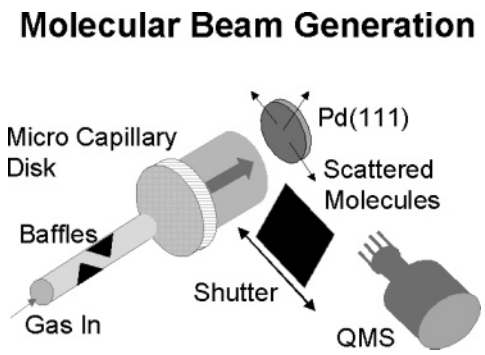


**Figure 1.** Schematic representation of molecular beam generation.

molecular beam doser setup (Figure 1), a quadrupole mass spectrometer (Pfeiffer, Prisma QMS 200 M3), a sputter ion gun (AG5000, VG Scientific), and sample preparation facilities. The mass spectrometer is kept out of the line-of-sight of the sample to avoid any angular desorption effects. The molecular beam doser consists of a 13 mm disk multichannel array made up of microcapillary glass tubes of 1 mm in length and 10 $\mu$m in diameter each (Collimated Holes Inc.). The NO gas-flux in the molecular beam ($F_{NO}$) is determined and controlled by the precision leak-valve opening and the backing gas pressure in the gas-manifold. A laterally movable stainless steel shutter, which is manually operated, was placed between the microcapillary doser and the Pd(111) crystal in order to interrupt the beam when desired (Figure 1). The Pd single crystal (Metal Crystals and Oxides Ltd., Cambridge, U.K.) was cut in the (111) direction and polished using standard procedures. It was mounted by spot-welding a 0.5 mm thick tantalum wire on the periphery of the crystal and connected to a pair of copper rods, which in turn were connected to a power-thermocouple feed-through. A K-type thermocouple was welded on the backside of the crystal and to the thermocouple leads of the feed-through. The above feed-through is connected to liquid nitrogen reservoir. The crystal can be cooled to about 100 K with liquid nitrogen or resistively heated to 1373 K. For the present experiments, the distance between the crystal and the beam doser is set to 5 mm.

The Pd(111) crystal surface was cleaned as described by Ramsier et al.[18] The procedure involves $Ar^+$ sputtering at 1000 K in a partial pressure of oxygen ($4 \times 10^{-8}$ Torr) for 60 min, followed by annealing for 30 min at 1000 K in $2 \times 10^{-7}$ Torr of oxygen, and, finally, flashing to 1200 K in a vacuum. This cycle was repeated several times, testing the cleanliness of the surface by monitoring CO and $CO_2$ during high-temperature flashing after oxygen adsorption at room temperature. Room-temperature NO adsorption and subsequent TPD experiments were also carried out, and the results (not shown) are in good agreement with results reported earlier,[17−19] ensuring surface cleanliness of Pd(111). However with subsequent NO dosing experiments, especially at high temperatures (above 500K), small amounts of $N_2$ and CO were observed during high temperature flashing, possibly indicating the subsurface diffusion of N and O atoms at high temperatures. Hence, after each set of high-temperature experiments the surface was cleaned by above $Ar^+$ sputtering procedure. For the present manuscript NO/Pd(111) studies between 300 and 525 K are being reported.

$^{15}NO$ (Air gas, 99% isotopically pure), $^{14}NO$, CO (99.9%), and $^{13}CO$ (Isotec) were used without any further purification. It is to be noted that the $^{15}NO$ contains about 1% of unlabeled $^{14}NO$. The purpose of using $^{13}CO$ and $^{15}NO$ is 2-fold: First it allows a clear identification of the possible products such as $^{13}CO_2$ (amu 45) and $^{15}N_2O$ (amu 46). In addition, these species can be distinguished from common background signals like $^{12}CO_2$ (amu 44). The second factor is related to the $^{13}CO$ employed to minimize the interference between background $^{12}CO$ and the main product of $N_2$ in the NO dissociation reaction. However, $^{14}NO$ (amu 30) present in the $^{15}NO$ interferes with the identification of $^{15}N_2$ (amu 30), and most of the experiments reported here are carried out with $^{14}NO$. However, cross-reference experiments were carried out with $^{15}NO$ too. Small amounts of $^{13}CO$ were present in the MBI chamber, adsorbing especially below 400 K. However, the adsorbed $^{13}CO$ does not interfere our experiments since CO is displaced by NO in the transient state of the subsequent experiments and can be detected easily.[35] Several test experiments have been carried out initially to probe all possible products of NO decomposition, including $N_2O$ and $NO_2$ under a variety of experimental conditions. Apart from nitrogen and nitrous oxide, no other nitrogen containing products were produced under any conditions. The mass spectrometer intensity was calibrated for NO by measuring the uptake on clean Pd(111) at 300 K, assuming a saturation coverage of 0.33 monolayers (ML) following Jacobi et al.[17] Different parameters ($s_{NO}$, $\Theta_{NO}$) were calculated by following the procedures given in ref 33.

## 3. Results and Discussion

**3.1. General Considerations.** The experimental procedure followed in a typical molecular beam dosing experiment is explained in Figure 2. For all experiments, the clean Pd(111) metal surface was kept at constant temperature and exposed to an effusive $^{14}NO$ molecular beam. All relevant gas-phase species formed are detected by QMS as a function of time. Figure 2 shows a typical set of kinetic data recorded during $^{14}NO$ exposure of Pd(111) at 465 K: At time $t = 5$ s, the molecular beam with a NO beam was allowed to enter the UHV chamber (Figure 1). With the shutter blocking the crystal, there is, however, no direct exposure to the $^{14}NO$ beam. Nonetheless, a small amount of $^{14}NO$ adsorption from the background cannot be prevented. After few seconds, at $t = 10$ s, the shutter was removed to allow the beam to directly impinge on the Pd(111) surface. An instantaneous decrease in the partial pressure of $^{14}NO$ for few seconds can be noticed as a result of $^{14}NO$ adsorption from the beam. This adsorption in the transient state continues until the surface is saturated with $^{14}NO$. The geometrical arrangements in our MBI[36] is such that about 25% of the beam is intercepted by the crystal and, hence, the drop in NO pressure upon shutter removal is relatively shallow; this is mainly to ensure an uniform beam profile over the entire crystal surface. A clear $N_2$ and $N_2O$ production in the transient state begins around $t = 15$ s can be seen, indicating the dissociation of $^{14}NO$ on the Pd(111) surface. Nitrogen desorption is evident at other temperatures also (Figure 4). However, the amount of $^{14}N_2O$ desorption is comparatively much lower than that of $N_2$. Amu 12 was also followed in all the experiments to ensure that there is no contribution from CO and $CO_2$.

The partial pressure of the $^{14}NO$ increases up to a new steady-state value, due to adsorption on UHV chamber walls;[11] however, it does not represent any change in the molecular beam characteristics. $^{14}NO$ adsorption was continued for at least 60 s before any steady-state measurements were made. Upon reaching the steady-state, the beam was blocked for about 30 s. During the beam blocking period in the steady state, an increase in the partial pressure of $^{14}NO$ (Figure 2) was observed clearly. Moreover, the sudden increase in the $^{14}NO$ partial pressure in the steady state upon closing the shutter can be attributed to the immediate desorption of $^{14}NO$, since the substrate temper-

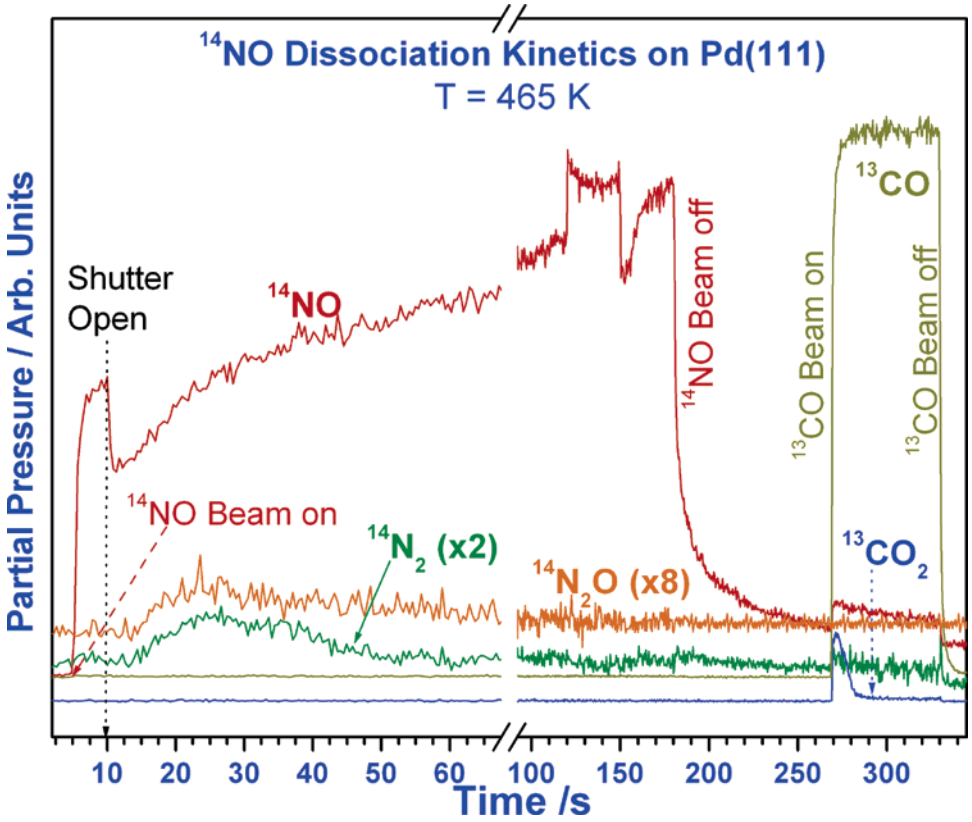


**Figure 2.** Experimental data from a typical isothermal kinetic test described in the text carried out with $^{14}NO$ at 465 K and subsequently the surface oxygen was titrated with $^{13}CO$ beam at the same temperature. Different mass traces are deliberately shifted to show the features clearly.

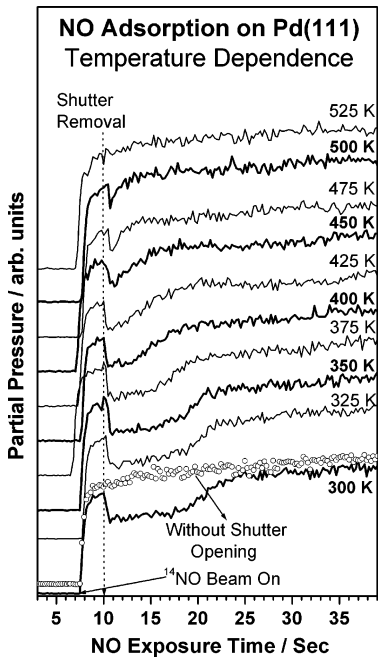


**Figure 3.** Temperature dependence of $^{14}NO$ adsorption on Pd(111) in the transient state on clean metal surface. Scattered data points (open circles) shown for 300 K are from the experiment carried out without opening the shutter to use as standard for background subtraction. Reference data has been shifted vertically for clarity.

ature is close to the NO desorption maximum of 500 K.[17−20] This result shows that there is a substantial $^{14}NO$ steady-state coverage established throughout the reaction period. $N_2$ and $N_2O$ desorption stops completely within a minute of starting of NO dosing and there is no change in the partial pressure of $N_2$ and $N_2O$ in the steady-state indicating that the NO dissociation activity does not sustain on its own. This is attributed to poisoning by dissociated atomic species, mainly oxygen atoms. It is also to be noted that the NO uptake after shutter removal in the steady state is nearly the same as that of NO uptake on clean Pd(111) in the transient state. This indicates that almost all nitrogen and NO desorb during the beam blocking period and the NO and nitrogen coverages are low.

A subsequent TPD shows no NO and a small nitrogen coverage. This is further supported by TPD results (in Figures 6). After turning off the NO beam, the $^{13}CO$ beam was switched on at $t = 270$ s. and constant temperature in order to titrate the surface oxygen species produced by NO dissociation. A clear production of $^{13}CO_2$ indicates the NO dissociation on Pd(111). The above CO dosing was carried out also to minimize the diffusion of oxygen into the subsurface and the bulk region. Finally, the $^{13}CO$ beam was shut off, and the chamber background pressure was allowed to return to normal before TPD experiments were performed at a heating rate of 5 K/s. The TPD results indicate a strongly temperature-dependent coverage of NO and small amount of nitrogen (Figure 6). As there is no desorption of nitrogen-related products above 550 K, the TPD experiments were stopped at 650 K. Subsequently, the Pd(111) crystal was flashed to 1000 K before the next dosing experiment.

**3.2. Temperature-Dependent NO Adsorption and Dissociation on Pd(111).** Figure 3 shows the temperature dependence of $^{14}NO$ adsorption on Pd(111) between 300 and 525 K at a constant $F_{NO} = 0.05$ ML/s. NO beam was turned on at $t = 7$ s followed by the shutter opening at $t = 10$ s; there is a clear decrease in the $^{14}NO$ partial pressure due to $^{14}NO$ adsorption on the Pd(111) surface at the shutter removal point. A number of reference experiments were made, in which the shutter was not at all opened and the data were used as background for those experiments reported in the manuscript for all the

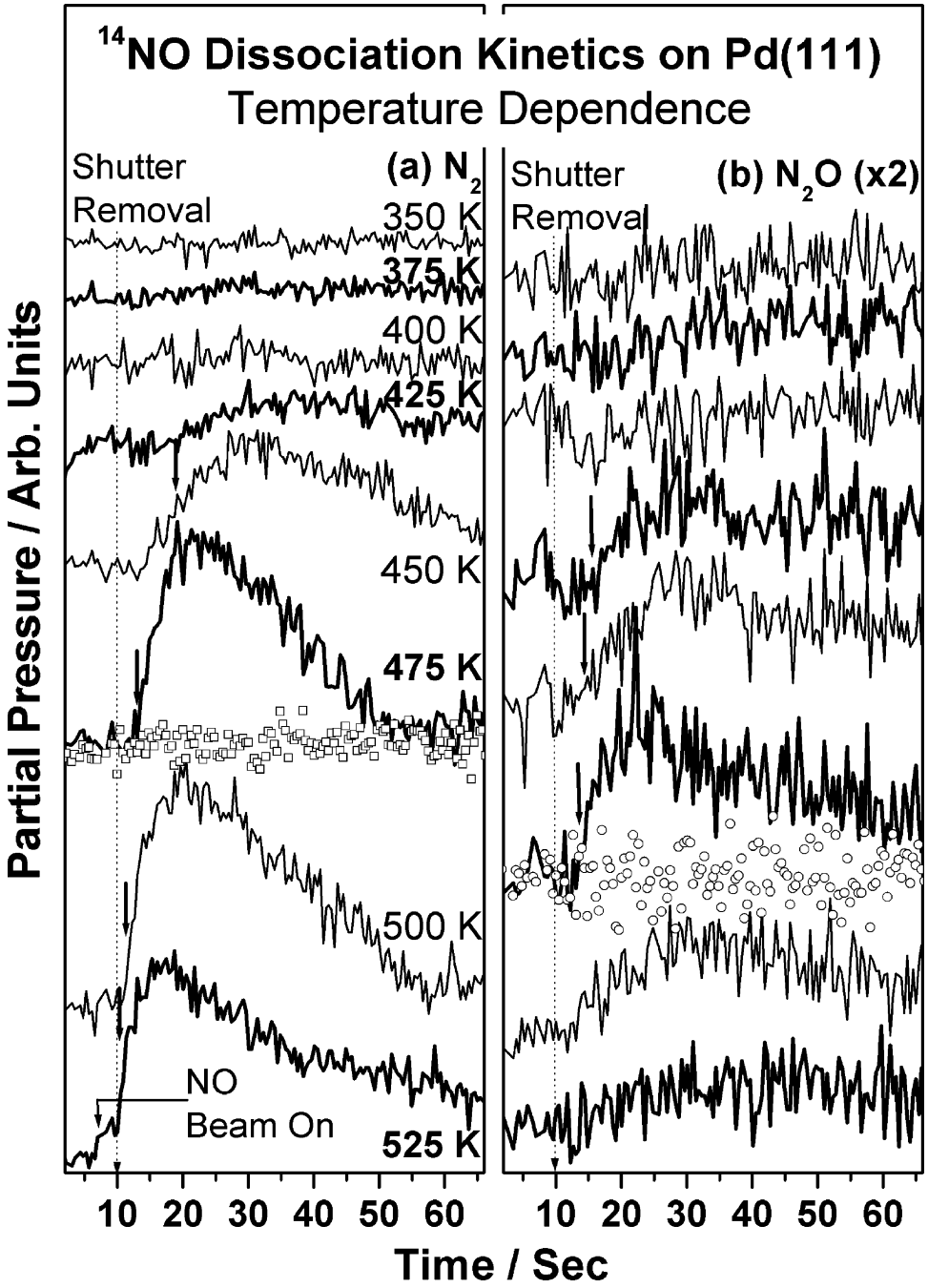


**Figure 4.** (a) $N_2$ and (b) $N_2O$ production from Pd(111) surface due to NO dosing at different temperatures. Note the maximum $N_2O$ production at 475 K and $N_2$ between 475 and 500 K. Solid arrows indicate the on-set of products desorption. Scattered data points shown for 475 K are from the experiment carried out without opening the shutter.

calculation purposes. One such reference experiment is shown in Figure 3 at 300 K. It is to be noted here that the above procedure is reliable than fitting with an exponential or quadratic equations. However, some background adsorption (about 5%) cannot be avoided,[33] and to reduce that contribution, a minimum time gap (2−3 s) was kept between the beam on and the shutter removal time. Further, the uniform beam profile over the crystal surface also ensures the pressure on the crystal surface is much higher than the background. At temperatures below 400 K, $^{14}$NO was continuously adsorbed at the same rate for a few seconds, before a gradual decrease occurs due to the surface reaching the saturation NO coverage ($\Theta_{NO}$) around $t = 20$ s. At and above 400 K, there is a gradually decreasing total NO adsorption capacity compared to the experiments between 300 and 350 K. The decreasing saturation coverage with increasing temperature is due to a reduction of the number of vacant sites, as a result of NO dissociation to N and O atomic species. It should also be noted that the initial NO adsorption probability remains constant immediately after the shutter removal at reaction temperatures between 300 and 425 K. The corresponding changes in the amu 28 and 44 traces (due to $^{14}N_2$ and $^{14}N_2O$) (Figure 4) provide a hint that, at least in part, the reduction in $\Theta_{NO}$ above 400 K is due to NO dissociation. There is a decrease in the initial and overall $^{14}$NO adsorption capacity above 450 K and no $^{14}$NO adsorption could be directly detected through pressure change at 525 K.

As far as product desorption is concerned, two temperature regimes can be observed in Figure 4: (i) NO adsorption without formation of any nitrogen containing products below 400 K and (ii) simultaneous $N_2$ and $N_2O$ production at ≥ 425 K. Above

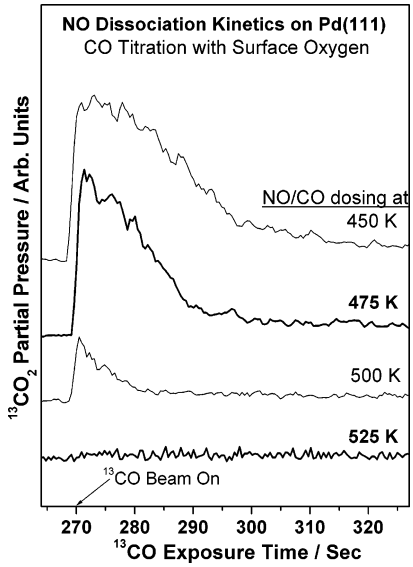


**Figure 5.** Surface oxygen due to NO dissociation on Pd(111) is titrated with $^{13}$CO beam at the same NO adsorption temperatures. Note the decrease in oxygen coverage ≥ 500 K is attributed to diffusion of oxygen into subsurface.

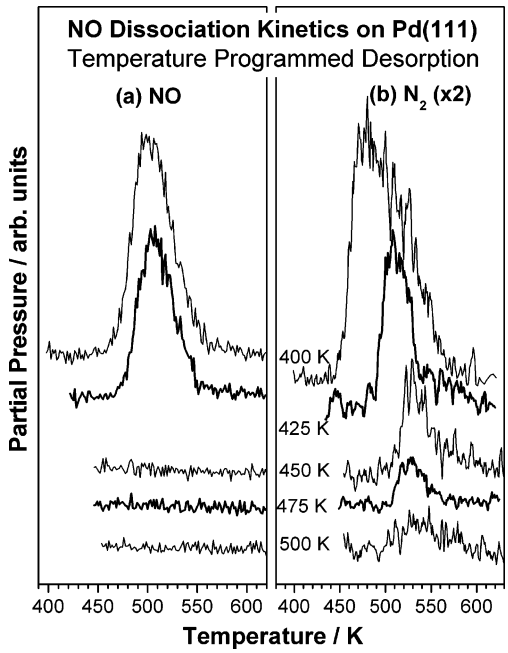


**Figure 6.** Representative results from the temperature-programmed desorption at a heating rate of 5 K/s carried out after the experiments described in Figures 3 and 4. NO dosing temperatures are given.

400 K, the formation of $N_2$ and $N_2O$ production becomes evident from the results shown in Figure 4. The reference experiments mentioned above, without removing the shutter, showed no considerable products formation is attributed to the low NO coverage under these conditions. It is interesting to compare the different kinetics of $N_2$ desorption and NO uptake. Indeed, a remarkable feature is the temporal behavior of the $N_2$ and $N_2O$ production between 425 and 500 K with a time delay observed for the onset of $N_2$ and $N_2O$ production, although NO uptake is observed at $t = 10$ s. This delay indicates the buildup of some nitrogen coverage. A finite time delay of about 6−7 s before the onset of $N_2$ and $N_2O$ production at 425 K decreases with increasing temperature (solid arrows in Figure 4). At 525 K, $N_2$ formation appears almost simultaneously with NO uptake upon shutter removal. Moreover, there is hardly any $N_2O$ formation. These observations can be interpreted in terms of an increasing NO dissociation probability, leading to a decreasing time gap between shutter removal and the onset of $N_2$ and $N_2O$ desorption at high temperatures. The above observations point toward the fact that $N_2$ and $N_2O$ desorption could be diffusion-controlled. In this case, the NO adsorption and dissociation steps could be faster than the production of $N_2$ and $N_2O$, under the above experimental conditions. Between 475 and 500 K, maximum nitrogen production can be clearly seen after shutter removal, indicating the fast dissociation of $^{14}$NO to a comparatively large extent. The total nitrogen formation rate goes through a maximum between 475 and 500 K, and at >500 K, a reduction in the reaction rate is observed. At 525 K, the nitrogen desorption continues for little longer than a minute. However a small amount of CO production is also inferred (through amu 12), possibly due to the interaction between mobile oxygen in the bulk/subsurface and carbon in bulk, along with $N_2$. At temperatures higher than 525 K, the CO production increases significantly and, hence, reliable NO dissociation experiments could not be performed. It is to be noted here that the oxygen migration and hence considerable concentration of oxygen in the subsurface reported recently by Leisenberger et al.[37] is in line with our observation.

A careful analysis of the products desorption traces in Figure 4 leads to the following four points: (a) There is a sudden rise in the $N_2$ and $N_2O$ production rate between 425 and 500 K, but after a time delay; the decreasing time delay with increasing temperature indicates a decrease in initial nitrogen buildup. (b) The slope of the leading edge of the $N_2$ (and $N_2O$) traces increases steeply with increasing temperature from 425 to 525 K. Also, a partial $N_2$ production through an $N_2O$ intermediate cannot be excluded on the basis of the experiments. (c) A clear decrease in $N_2O$ production at >475 K with no $N_2O$ at 525 K indicates, again a change in overall kinetics and mechanism. (d) The selectivity for $N_2$ production is 5−10 times higher than for $N_2O$, depending on the temperature. In this respect, the presence of coadsorbed oxygen due to NO dissociation can be expected to be an important factor. However, it is difficult to quantify this effect, especially due to the onset of subsurface diffusion and possible surface oxidation around 475 K (see next section). Also on rhodium surfaces, it has been confirmed that coadsorption of oxygen and nitrogen leads to $N_2$ desorption at lower temperatures as compared to $N_2$ desorption from the N-only containing Rh surfaces.[38−40] The effect was attributed to repulsive interactions between N and O atoms on the surface. Indeed, oxygen pre-dosage was shown to completely inhibit NO dissociation,[16] indicating that similar effect may be operative on Pd(111). Another interesting aspect is the dynamic NO adsorption−desorption behavior observed on the Pd(111) surface in the steady-state. Although $N_2$ and $N_2O$ desorption stops in the transient state, NO adsorption−desorption continues, as long as the NO beam is maintained for the reaction temperatures below 500 K. Remarkably, the extent of NO adsorption in the steady-state after shutter removal at $t = 150$ s is similar to that of the NO uptake on clean Pd(111) surface at the beginning (see Figure 2). Similar observations were made down to 350 K (data not shown). This directly suggests that the oxygen and nitrogen coverage due to NO dissociation does not affect the NO adsorption in a significant manner, and hence, it might not play any important role in the overall kinetics of NO dissociation, at least below 500 K. This is in sharp contrast to the NO dissociation behavior on supported Pd particles studied recently.[28,29] The complete loss of the NO adsorption capacity in the latter case at temperatures at >375 K supports the hypothesis

that NO dissociation on the particles is strongly dominated by defect sites.

At ≥500 K on Pd(111), the steady-state NO coverage in the dynamic adsorption−desorption equilibrium decreases drastically, indicating fast desorption. Furthermore, it is likely that the substantial drop in $N_2O$ production above 500 K is related to the rapidly decreasing NO coverage in this temperature region (see section 3.6).

**3.3. Surface Oxygen Coverage and Oxygen Diffusion into Subsurface/Bulk.** Figure 5 shows the results on the surface oxygen titration with $^{13}CO$ beam after the NO adsorption experiments, as explained in Figure 2. CO dosing was carried out at the same reaction temperature as that of NO adsorption. $^{13}CO_2$ production was observed at temperatures between 400 and 475 K. However, $CO_2$ desorption decreases sharply at 500 K and no $CO_2$ was observed at 525 K, despite nitrogen desorption observed in the transient state, shown in Figure 4. This is attributed mainly to subsurface diffusion of oxygen and surface oxidation of Pd(111). As noted earlier, there is a small amount of $^{12}CO$ production along with $N_2$ at 525 K in the NO adsorption experiments. Further, there is some carbon oxide formation while flashing to 1000 K, after reaction. Above observations supports the hypothesis of oxygen diffusion into the subsurface and surface oxide formation. Desorption of no or very small amount of molecular oxygen above 700 K in TPD[20,21] due to NO dissociation on a variety of Pd surfaces, including Pd(311) where NO dissociation is largest, unambiguously hints the disappearance of oxygen from the surface and it has been attributed to oxygen diffusion and supports our above conclusion. Leisenberger et al.[37] observed oxygen diffusion into the near surface region at 523 K and in good agreement with our results.

Recently, surface oxide formation on Pd(111) has been investigated experimentally in great detail.[41−45] Also, the oxidation of Pd surfaces has been investigated theoretically[44] and shows that subsurface oxygen is just a precursor to surface oxidation. Decreasing the $CO_2$ signal at 500 K in our results may also be due to a reduced reaction probability of CO and the inability to strongly adsorb CO due to the oxidized palladium surface. It is to be noted that the more oxidized Pd surface and PdO are unreactive toward CO, as found by Zhang and Altmann.[42] Indeed the amount of $CO_2$ desorption at 475 K is somewhat lower than at 450 K, indicating that surface oxidation may begin around 475 K, in accordance with adsorption studies on Pd(111) at elevated temperatures.[41,42] The complex interaction of the Pd surfaces with oxygen significantly complicates the kinetic analysis, especially at temperatures above 475 K. However, sustainable $CO_2$ production in NO + CO reactions on Pd(111) up to 625 K[23,35] suggests that surface oxide formation and subsurface diffusion may be strongly suppressed in the presence of CO as a reducing agent.

**3.4. Temperature-Programmed Desorption Studies of NO/Pd(111).** Figure 6 shows the TPD of NO and $N_2$ species recorded after the above dosing experiments. No significant $N_2O$ was observed. NO desorbs between 450 and 550 K, in good agreement with the earlier TPD results.[16−19] Gradual decrease in the quantity of NO desorbed is observed in the TPD from the NO dosing experiments conducted above 300 K (not shown). Between 300 and 325 K, no change in NO coverage was observed in TPD (as well as NO uptake in dosing) experiments, suggesting that the $\gamma$-saturation coverage[16−19] is retained. However, the NO yield in TPD decreases linearly from 0.33 to 0 ML between 300 and 325 and 450 K dosing temperatures, respectively. Nonetheless, the temperature-dependent NO dosing

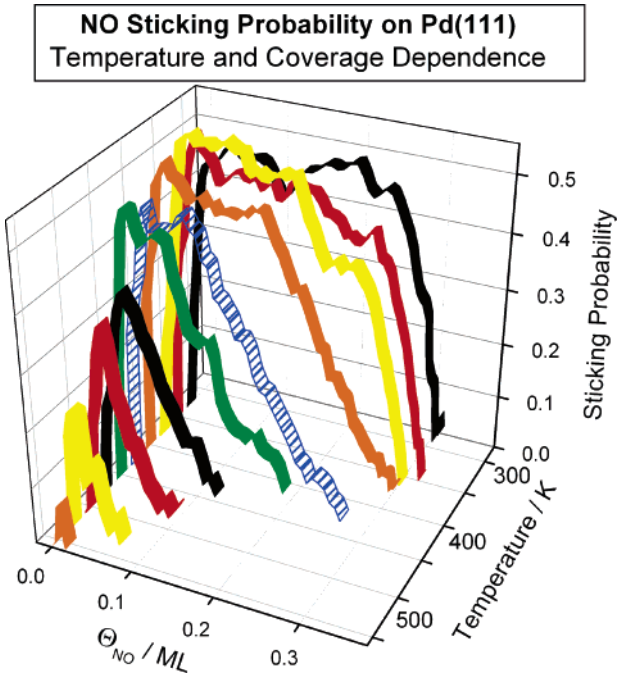


**Figure 7.** Temperature dependence of $\Theta_{NO}$ coverage and sticking coefficient calculated from the NO uptake data in Figure 3. Note the same initial sticking coefficient is maintained between 300 and 425 K up to about 80% saturation coverage for adsorption temperatures at 300 and 325 K

experiments indicate NO uptake on the surface at adsorption temperature <500 K. It may be recalled here that the NO uptake on clean Pd(111) at the beginning of the experiment as well as in the steady-state after temporary blocking is almost the same (Figure 2 − note the change in *x*-axis scale after the break). This shows that there is complete desorption of NO with no beam at temperatures >425 K on the time scale of the experiment.

TPD results display a decrease in nitrogen desorption, suggesting that the atomic nitrogen coverage decreases with increasing temperature. However, the nitrogen coverage seen on Pd(111) in the TPD is ≤0.06 ML and comparable to that of nitrogen coverage observed after NO + CO reaction on Pd(111).[35] Nonetheless, the nitrogen coverage is much lower than that observed on Rh(111)[11,46] after NO and/or NO + CO reactions.

**3.5. Sticking Coefficient of NO on Pd(111).** Figure 7 shows the temperature and $\Theta_{NO}$ dependence of $s_{NO}$ on Pd(111), by adopting the method employed in refs 33 and 47−49. Briefly, $s_{NO}$ is directly proportional to the change in pressure due to NO uptake on Pd(111) after shutter removal with respect to the total pressure if there was no adsorption. Furthermore, $s_{NO}$ (0.5) is inversely proportional to the fraction of the beam intercepted, which is 0.25 in the present case. Estimated error margin of $s_{NO}$ values from the uptake measurements is up to 5% and should be considered for any purpose. A time evolution of $s_{NO}$ was calculated first from the experimental data, given in Figure 3, and converted in terms of increasing $\Theta_{NO}$. The initial $s_{NO}$ is constant between 300 and 425 K and decreases at temperatures higher than 425 K. A maximum of $s_{NO} = 0.5$ was observed at low temperatures between 300 and 350 K on clean Pd(111) up to 70−80% of the saturation coverage. This behavior is typical of precursor-mediated adsorption. At high temperature, the plateau becomes smaller due to faster desorption and phenomenologically a description of $s_{NO}$ on the basis of a Langmuir model becomes more appropriate. Very similar trend

in $s_{NO}$ on Pd(110) surface was reported by Sharpe and Bowker[21] and indicates the lifetime of chemisorbed NO species decreases linearly with increasing temperature on Pd(111) and Pd(110).

**3.6. Reaction Mechanism.** The isothermal experimental results in a molecular beam setup provide some new insights into the mechanism for the thermal dissociation of NO on Pd(111) surfaces. Earlier reports[18,25] suggested the main elementary steps of the reaction in this system are

$$NO_{(g)} \leftrightarrow NO_{(ads)} \quad (1)$$

$$NO_{(ads)} \rightarrow N_{(ads)} + O_{(ads)} \quad (2)$$

$$N_{(ads)} + N_{(ads)} \rightarrow N_{2(g)} \quad (3)$$

$$N_{(ads)} + NO_{(ads)} \rightarrow N_2O_{(g)} \quad (4)$$

$$O_{(ads)} \xrightarrow{>475\ K} O_{(sub-surface)} + O_{(surface-oxide)} \quad (5)$$

Although the above mechanism may appear simple, there are few complications that have not been resolved until now. In particular, TPD experiments show weakly and strongly adsorbed nitrogen peaks at 450 K and between 545 and 595 K, respectively, by Goodman et al.;[23] however only a minor $N_2$ peak at 500 K was observed by several other groups.[16,18,22] TPD results of Nakamura et al.[20] and Wickham et al.[50] show no evidence of NO dissociation on Pd(111). In contrast, pronounced $N_2$ desorption was observed at 670 K by Conrad et al.[17] Sugai et al.[19] also shows through Auger electron spectroscopy that surface-bound N remains on the surface as high as 700 K. Although present isothermal experiments may not be compared directly to the earlier TPD results due to the different reaction conditions in a molecular beam setup, certain valid conclusions may be derived as discussed in the following.

Our present results shows that, indeed, there is NO dissociation activity on Pd(111), which leads to dominant production of $N_2$ and minor $N_2O$ production between 400 and 500 K and exclusive $N_2$ production above 500 K. Nevertheless, some NO dissociation activity is possible from the defect sites (step sites) and cannot be ruled out. A substantial NO coverage on Pd(111) is observed between 400 and 500 K in the dynamic adsorption−desorption equilibrium and it is not strongly affected by the presence of N and O atomic species. This result is in general agreement with the observation of comparable coverages of NO coverage via high-resolution electron energy loss spectroscopy measurements by Ramsier et al.[18] This suggest that the NO adsorption [eq 1] cannot be the rate-determining step (RDS), at least below 500 K. Post-mortem TPD experiments shows that there is only one $N_2$ desorption peak with a peak maximum around 500−530 K and in good agreement with majority of earlier reports.[16,18,22] New observation of nitrogen desorption show some delay with respect to NO uptake, indicating that atomic nitrogen recombination to gaseous $N_2$ could have large degree of rate control. The delay in the nitrogen desorption below 500 K may also be explained in terms of the necessity of a critical surface N concentration before their average interatomic distances are short enough, so that they can interact to form $N_2$ molecule. Nonetheless, repulsions among the dissociated atomic species lowers desorption barrier as well as the strength of adsorption and hence it should also be taken into account. However, as the temperature increases the diffusion rate of atomic nitrogen also increases and hence a decrease in the initial delay as well as N-buildup and instant $N_2$ production can be observed at 500−525 K. In fact, the common leading edge of the isothermal kinetic runs, below 525 K, is expected for a two-dimensional diffusion-limited reactions.[46] Similar results of a time gap between NO uptake and nitrogen formation and the repulsive interactions between the atomic species has been observed and reported on Pd(110),[21] Rh(110),[39] and Rh(111)[11,39,46] surfaces. Furthermore, on the basis of the observation of a significant NO coverage and nitrogen buildup it can also not be excluded that the $N_2$ formation, at least in part, might be through an $N_2O$ intermediate also. Indeed, a similar slope in the leading edges of $N_2$ and $N_2O$ desorption kinetics supports this view; nonetheless, further support is necessary. The small nitrogen coverage observed in the TPD after reactions above 425 K indicates that the oxygen could exert repulsive interactions with nitrogen, providing an additional driving force for $N_2$ desorption. Nevertheless, the high rate of subsurface diffusion of oxygen and surface oxide formation around 525 K may change the nature of the surface and affect the overall kinetics. As the nitrogen coverage decreases drastically >500K along with an increase in NO desorption rate, both nitrogen recombination and adsorption are not expected to contribute substantially to the rate control. However, NO dissociation might play a significant role toward the overall kinetics at temperatures higher than 525 K.

Indeed, fast $CO_2$ production below 525 K in NO + CO reactions on Pd(111) supports the relatively fast NO dissociation.[35] The complete stopping of NO dissociation in the steady-state is attributed to the sizable oxygen coverage observed through CO titration and it is in correspondence with the observation of Schmick et al.[16] and Henry et al.[25] that coadsorbed oxygen eliminates NO dissociation. Also on supported Pd particles, we have recently observed large oxygen coverages after NO dissociation, together with small amounts of N adsorbed at specific sites on the particles.[28,29]

## 4. Conclusions

A simple molecular beam instrument fabricated for gas-phase surface reaction studies on metal surfaces is described. The instrument is employed to probe NO adsorption and its dissociation on Pd(111) surface through isothermal kinetic experiments between 300 and 525 K. Molecular NO adsorption was observed at ≤400 K. The adsorption kinetics indicate that NO dissociation starts on Pd(111) surfaces at around 400 K. NO dissociation to $N_2$ and $N_2O$ was observed clearly in the transient state at temperatures ≥425 K. Major amounts of nitrogen desorption were found along with a minor amount of $N_2O$ desorption, in agreement with earlier results from TPD. The decrease in the time delay between nitrogen desorption onset and the shutter removal at increasing temperature suggests that nitrogen formation occurs through a diffusion-controlled mechanism and it could be partly rate limiting, at least below 500 K. The rate of $N_2$ formation does not follow that of NO uptake. The adsorption−desorption equilibrium of NO is established in the presence of NO beam, indicating substantial NO coverages below 500 K. Oxygen diffusion into the subsurface sites and surface oxide formation starts around 475 K and increases significantly above 525 K. Sticking coefficient measurements show $s = 0.5$ for NO adsorption between 300 and 350 K up to high coverage, indicating the precursor mediated adsorption. $s_{NO}$ decreases with increasing coverage and temperature. The present molecular beam experiments on NO dissociation throw more light than the earlier conventional TPD experiments.

**Acknowledgment.** The authors are grateful to Professor H.-J. Freund, FHI, Berlin, for his keen interest, and support for the present work. We thank the reviewers for constructive

suggestions. C.S.G. thanks Dr. S. Sivaram, Director, NCL, for his constant encouragement. Financial support to this project by the Volkswagen Foundation (Program of Partnership, "The Mechanism and Kinetics of NO Reduction Reactions on Noble Metal Surfaces−From Single Crystal Surfaces to Supported model Catalysts") is gratefully acknowledged. C.S.G. thanks the Alexander von Humboldt (AvH) foundation for partial financial support during the molecular beam facility fabrication at NCL, Pune, India, under the instrument donation program to the former AvH fellows. C.S.G. also thanks the NCL for an in-house project (MLP 004226). K.T. thanks CSIR, New Delhi, for senior research fellowship.

## References and Notes

(1) Taylor, K. C. *Catal. Rev. Sci. Eng.* **1993**, *3*, 457.
(2) Shelef, M.; Graham, G. W. *Catal. Rev. Sci. Eng.* **1994**, *36*, 433.
(3) Kreuzer, T.; Lox, S. E.; Lindner, D.; Leyrer, J. *Catal. Today* **1996**, *29*, 17.
(4) Jobson, E. *Top. Catal.* **2004**, *28*, 191.
(5) Tagliaferri, S.; Kõppel, R. A.; Baiker, A. *Stud. Surf. Sci. Catal.* **1998**, *116*, 61. van Yperen, R.; Lindner, D.; Mussmann, L.; Lox, E. S.; Kreuzer, T. *Stud. Surf. Sci. Catal.* **1998**, *116*, 51.
(6) Berndt, H.; Schutze, F. W.; Richter, M.; Sowade, T.; Grunert, W. *Appl. Catal., B* **2003**, *40*, 51. Olsson, L.; Persson, H.; Fridell, E.; Skoglundh, M. *J. Phys. Chem. B* **2001**, *105*, 6895.
(7) Takahashi, N.; Shinjoh, H.; Iijima, T.; Suzuki, T.; Yamazaki, K.; Yokota, K.; Suzuki, H.; Miyoshi, N.; Matsumoto, S.; Tanizawa, T.; Tanaka, T.; Tateishi, S.; Kasahara, K. *Catal. Today* **1996**, *27*, 63.
(8) Salasc, S.; Skoglundh, M.; Fridell, E. *Appl. Catal., B* **2002**, *36*, 145.
(9) Holles, J. H.; Davis, R. J.; Murray, T. M.; Howe, J. M. *J. Catal.* **2000**, *195*, 193.
(10) Martinez-Arias, A.; Fernandez-Garcia, M.; Hungria, A. B.; Iglesias-Juez, A.; Duncan, K.; Smith, R.; Anderson, J. A.; Conesa. J. C.; Soria, J. *J. Catal.* **2001**, *204*, 238.
(11) Gopinath. C. S.; Zaera, F. *J. Catal.* **1999**, *186*, 387. Zaera. F.; Gopinath, C. S. *J. Chem. Phys.* **1999**, *111*, 8088.
(12) Zhdanov. V. P.; Kasemo, B. *Surf. Sci. Rep.* **1997**, *29*, 31.
(13) Peden, C. H. F.; Goodman, D. W.; Blair, D. S.; Berlowitz, P. J.; Fisher, G. B.; Oh, S. H. *J. Phys. Chem.* **1988**, *92*, 1563.
(14) Permana, H.; Ng, K. Y. S.; Peden, C. H. F.; Schmieg, S. J.; Lambert, D. K.; Belton, D. N. *J. Catal.* **1996**, *164*, 194.
(15) Borg, H. J.; Reijerse, J. F. C.-J. M.; van Santen, R. A.; Niemants-verdriet, J. W. *J. Chem. Phys.* **1994**, *101*, 10052.
(16) Schmick, H.-D.; Wassmuth, H.-W. *Surf. Sci.* **1982**, *123*, 471.
(17) Conrad, H.; Ertl, G.; Küppers, J.; Latta, E. E. *Surf. Sci.* **1977**, *65*, 235. Bertolo, M.; Jacobi, K.; Nettesheim, S.; Wolf, M.; Hasselbrink, E. *Vacuum* **1990**, 76. Bertolo, M.; Jacobi, K. *Surf. Sci.* **1990**, *226*, 207.
(18) Ramsier, R. D.; Gao, Q.; Neergaard Waltenburg, H.; Lee, K.-W.; Nooij, O. W.; Leerts, L. Yates, J. T., Jr. *Surf. Sci.* **1994**, *320*, 209. Ramsier, R. D.; Gao, Q.; Neergaard Waltenburg, H.; Yates, Jr., J. T. *J. Chem. Phys.* **1994**, *100*, 6837.
(19) Sugai, S.; Watanabe, H.; Kioka, T.; Miki, H.; Kawasaki, K. *Surf. Sci.* **1991**, *259*, 109.
(20) Nakamura, I.; Fujitani, T.; Hamada, H. *Surf. Sci.* **2002**, *514*, 409.
(21) Sharpe, R. G.; Bowker, M. *Surf. Sci.* **1996**, *360*, 21.
(22) de Wolf, C. A.; Nieuwenhuys, B. E. *Surf. Sci.* **2002**, *196*, 469.
(23) Rainer, D. R.; Vesecky, S. M.; Koranne, M.; Oh, W. S.; Goodman, D. W. *J. Catal.* **1997**, *167*, 234. Ozensoy, E.; Hess, C.; Goodman, D. W. *J. Am. Chem. Soc.* **2002**, *124*, 8524.
(24) Piccolo, L.; Henry, C. R. *Appl. Surf. Sci.* **2000**, *162*−*163*, 670.
(25) Piccolo, L.; Henry, C. R. *Surf. Sci.* **2000**, *452*, 198. Prevot, G.; Henry, C. R. *J. Phys. Chem. B.* **2002**, *106*, 12191.
(26) Seldmair, C.; Seshan, K.; Jentys, A.; Lercher, J. A. *J. Catal.* **2003**, *214*, 308.
(27) Hirsimaki, M.; Valden, M. *J. Chem. Phys.* **2001**, *114*, 2345.
(28) Joha'nek, V.; Schauermann, S.; Laurin, M.; Libuda, J.; Freund, H.-J. *Angew. Chem., Int. Ed.* **2003**, *42*, 3035.
(29) Johanek, V.; Schauermann, S.; Laurin, M.; Gopinath, C. S.; Libuda. J.; Freund, H.-J. *J. Phys. Chem. B* **2004**, *108*, 14244.
(30) D'Evelyn, M. P.; Madix, R. J. *Surf. Sci. Rep.* **1984**, *3*, 413.
(31) Asscher, M.; Somorjai, G. A. In *Atomic and Molecular Beam Methods*; Scoles, G., Ed.; Oxford University Press: Oxford, U.K., 1988; Vol. 2, p 489.
(32) Rettner, C. T.; Auerbach, D. J.; Tully, J. C.; Kleyn, A. W. *J. Phys. Chem.* **1996**, *100*, 13021.
(33) Liu, J.; Xu, M.; Nordmeyer, T.; Zaera, F. *J. Phys. Chem.* **1995**, *99*, 6167.
(34) Libuda, J.; Meusel, I.; Hartmann, J.; Freund, H.-J. *Rev. Sci. Instrum.* **2000**, *71*, 4395.
(35) Thirunavukkarasu, K.; Thirumoorthy, K.; Libuda, J.; Gopinath, C. S. *J. Phys. Chem. B* **2005**, *109*, 13272.
(36) Thirunavukkarasu, K.; Gopinath, C. S. Unpublished work.
(37) Leisenberger, F. P.; Koller, G.; Sock, M.; Surnev, S.; Ramsey, M. G.; Netzer, F. P.; Klötzer, B.; Hayek, K. *Surf. Sci.* **2000**, *445*, 380.
(38) Belton, D. N.; DiMaggio, C. L.; Ng, K. Y. S. *J. Catal.* **1993**, *144*, 273 and references therein.
(39) Zaera. F.; Gopinath, C. S. *J. Chem. Phys.* **2001**, *116*, 1128 and references therein.
(40) Bowker, M.; Guo. Q.; Joyner, R. W. *Surf. Sci.* **1991**, *257*, 33.
(41) Klötzer, B.; Hayek, K.; Konvicka, C.; Lundgren, E.; Varga, P. *Surf. Sci.* **2001**, *482*, 237.
(42) Zheng, G.; Altman, E. I. *Surf. Sci.* **2000**, *462*, 151. Zheng, G.; Altman, E. I. *Surf. Sci.* **2002**, *504*, 253. Zheng, G.; Altmann, E. I. *J. Phys. Chem. B* **2002**, *106*, 1048.
(43) Bondzie, V. A.; Kleban, P. H.; Dwyer, D. J. *Surf. Sci.* **2000**, *465*, 266.
(44) Todorova, M.; Reuter, K.; Scheffler, M. *J. Phys. Chem. B* **2004**, *108*, 14477. Lundgren, E.; Gustafson, J.; Mikkelsen, A.; Andersen, J. N.; Stierle, A.; Dosch, H.; Todorova, M.; Rogal, J.; Reuter, K.; Scheffler, M. *Phys. Rev. Lett.* **2004**, *92*, 046101.
(45) Teschner, D.; Pestryakov, A.; Kleimenov, E.; Hävecker, M.; Bluhm, H.; Sauer, H.; Knop-Gericke, A.; Schlögl, *J. Catal.* **2005**, *230*, 186.
(46) Aryafar, M.; Zaera, F. *J. Catal.* **1998**, *175*, 316.
(47) Madey, T. E. *Surf. Sci.* **1972**, *33*, 355.
(48) Jiang, L. Q.; Koel, B. E. J. *Phys. Chem.* **1992**, *96*, 8694.
(49) Campbell, C. T.; Valone, S. M. *J. Vac. Sci. Technol.* **A 1985**, *3*, 408.
(50) Wickham, D. T.; Banse, B. A.; Koel, B. E. *Surf. Sci.* **1991**, *243*, 83.